Available online at www.sciencedirect.com
SCIENCE DIRECT®
Scripta Materialia 51 (2004) 1005–1010
Scripta MATERIALIA
www.actamat-journals.com

Structure and transition of eutectic $(Mg,Al)_2Ca$ Laves phase in a die-cast Mg–Al–Ca base alloy

A. Suzuki *, N.D. Saddock, J.W. Jones, T.M. Pollock

Department of Materials Science and Engineering, University of Michigan, 3062 H.H. Dow 2300 Hayward St., Ann Arbor, MI 48109, USA

Received 11 May 2004; received in revised form 13 July 2004; accepted 14 July 2004
Available online 6 August 2004

Abstract

The crystal structure of a eutectic $(Mg,Al)_2Ca$ Laves phase in as-cast AXJ530 (Mg–5Al–3Ca–0.15Sr) was identified as C36 by electron diffraction analysis. The C36 phase transformed to C15(Al_2Ca) during annealing at 573 K. The orientation relationship for the C15 and C36 phases is reported.

Keywords: Magnesium alloys; Laves phase; Electron diffraction; Crystal structure

1. Introduction

There is a growing effort to develop high temperature structural magnesium alloys for weight reduction in automotive components to achieve high fuel efficiency. The improvement of creep resistance without raising material cost is a key issue for alloy development. Recently, the addition of Ca, which is a lower cost and weight element than rare-earth elements, to Mg–Al base alloys has been found to be effective in improving high temperature strength in Mg–(3–9)wt%Al [1], AZ81(Mg–8wt%Al–1wt%Zn) [2] and AM50(Mg–5wt%Al–0.3wt%Mn) [3]. Further addition of a small amount of Sr (AXJ alloys) is also reported to improve creep resistance with properties equal or superior to that of AE42 [4,5].

Die-cast magnesium alloys usually consist of dendritic α-Mg grains with intermetallic phase(s) in the interdendritic region. The high-temperature deformation of Mg–Al based alloys is considered to be controlled by dislocation motion in α-Mg grains at higher stress and grain boundary sliding at lower stress [4,6]. Moreno et al. [7] pointed out that grain boundary strengthening and stability, as well as solid solution and precipitation strengthening in α-Mg grains, are the important factors for optimization of the high temperature strength of fine-grained die-cast alloys. Since these magnesium alloys are to be used in the as-cast form in automotive components, microstructure evolution is unavoidable during elevated temperature service, especially near grain boundaries where higher alloying element concentration arises during solidification.

In Mg–Al–Ca based alloys, Mg_2Ca and/or Al_2Ca phases are known to form in the interdendritic region in preference to the $Mg_{17}Al_{12}$ phase observed in the binary system [6]. Mg_2Ca and Al_2Ca are Laves phases with crystal structures of C14(hexagonal) and C15(cubic), respectively. There have been several investigations of the phases present in near-grain boundary regions, but there is presently no consensus. Ninomiya et al. [1] examined Mg–(3–9)wt%Al–(1–5)wt%Ca alloys by X-ray diffraction and reported that both Mg_2Ca and Al_2Ca phases exist in alloys where the Ca/Al mass ratio

* Corresponding author. Tel.: +1 734 763 1406; fax: +1 734 615 5168.
E-mail address: akanes@engin.umich.edu (A. Suzuki).

1359-6462/$ - see front matter © 2004 Acta Materialia Inc. Published by Elsevier Ltd. All rights reserved.
doi:10.1016/j.scriptamat.2004.07.011

is more than 0.8 and that only the Al_2Ca phase exists in alloys with Ca/A1 < 0.8 in both the as-cast state and at 673 K. On the other hand, Luo et al. [4] examined AC53(Mg–4.5%Al–3%Ca) alloy which has Ca/Al ratio of 0.67 by TEM, and found that the eutectic region among α-Mg grains consisted of α-Mg and a ternary compound of $(Mg,Al)_2Ca$ with hexagonal structure. Ozturk et al. [8] also examined the same AC53 alloy by X-ray diffraction and suggested that the eutectic compound is $(Mg,Al)_2Ca$ with C14 structure in the as-cast state but it changes into Al_2Ca(C15) after aging at 643 K. In addition, Ameroun et al. [9] recently pointed out the existence of another Laves phase with C36 structure in the pseudo-binary system between Mg_2Ca and Al_2Ca by X-ray diffraction and first-principles calculations. Ternary phase equilibria have been studied by both experiment [10] and thermodynamic calculations [8,11,12]. However, it is important to understand what phases exist in the non-equilibrium as-cast state and how phases evolve at elevated temperatures.

In this study, a modified Mg–Al–Ca alloy with a small amount of Sr (AXJ530) has been investigated, focusing on the crystal structure of the intermetallic compounds in the eutectic regions surrounding the α-Mg grains. Intermetallic phases present in the as-cast material and their stability at elevated temperature have been examined in detail by transmission electron microscopy (TEM).

2. Experimental procedures

The AXJ530 alloy used in this study was supplied by General Motors and had a composition of Mg–4.52Al–2.98Ca–0.14Sr–0.25Mn(wt%). To fabricate this alloy, commercial AM50 alloy was used as a base and pure Ca and an Al–10wt%Sr alloy were added to achieve the desired composition. The alloy was melted at 950 K, and after high speed stirring for 3.6 ks, cold-chamber die-casting with a die temperature at 400 K was utilized to produce cylindrical shaped samples 6 mm in diameter and 25 mm in length.

A portion of the as-cast specimen was aged at 573 K for 360 ks, followed by a water quench. An aging treatment was conducted by sealing the sample in a quartz capsule that was argon back-filled after evacuation. After holding the capsule in the furnace, the sample was quenched into water quickly by breaking the capsule.

The as-cast and aged samples were examined by TEM. TEM discs 0.12 mm in thickness and 3 mm in diameter were cut from near the center of the die-cast specimen and mechanically polished, followed by twin-jet electron polishing in a solution of methanol with 8 vol.% perchloric acid at 243 K. Subsequently, low-angle ion milling was employed to remove the surface oxide layer introduced during jet polishing. A Phillips CM12 microscope was used in this study.

3. Results

3.1. Crystal structure of the eutectic compound

Fig. 1 shows TEM bright field image (BFI) of as-cast AXJ530. The typical microstructure contained equiaxed grains with a grain size of 5–20 μm. A eutectic microstructure was observed at the periphery of the α-Mg grains, especially at the triple points. The extent of the eutectic region was several μm, and the width of the individual eutectic phases was about 150 nm. The phases with bright and dark contrast correspond to α-Mg and the intermetallic compound, respectively.

Detailed electron diffraction analysis of the eutectic phases has been conducted. Fig. 2 shows BFIs and corresponding selected area diffraction patterns (SADPs) taken from the eutectic regions. Fig. 2(b) is the SADP taken from the region shown in (a), and Fig. 2(c) is obtained in the same region after rotating the sample by 30° with fixed reciprocal lattice vector $\mathbf{g}_1$. Fig. 2(e) and (f) are taken from the region shown in (d), and (f) was obtained by about 25° rotation from (e) with fixed $\mathbf{g}_2$. The diffraction pattern (e) has an equilateral-hexagonal arrangement of reflections. In addition, $\mathbf{g}_2$ is the common reciprocal lattice vector in (c) and (e). These facts indicate that the eutectic compound has a hexagonal base structure, and the incident beam directions of (b), (c) and (e) are $10\bar{1}0$, $2\bar{1}\bar{1}0$ and 0001, respectively. Note that strong streaks are observed in (b) and (c) along $\mathbf{g}_1$. All of the obtained diffraction patterns were consistent with those of dihexagonal C36 structure. The reflections marked with white arrowheads in (c) and (f) are extra with respect to the C14 structure. In particular, the existence of reflections between 0000 and 0002 in (c) indicates that the unit cell of the C36 is twice that of the C14 structure along the *c*-axis,

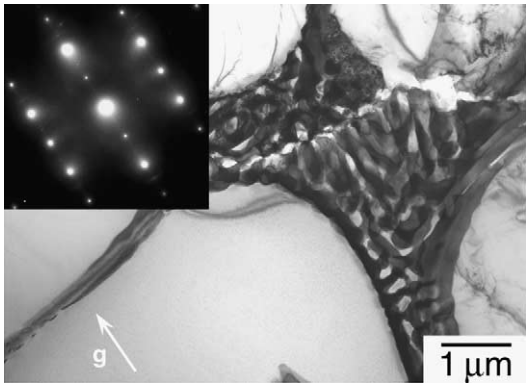

Fig. 1. TEM BFI of as-cast sample ($\mathbf{B} = 2\bar{1}\bar{1}0$).

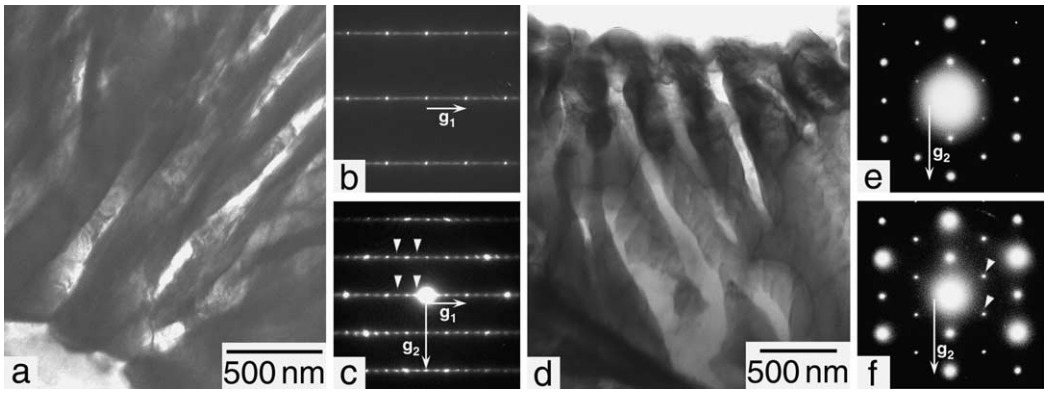

Fig. 2. TEM BFIs and SADPs taken from the eutectic regions: (a) BFI ($\mathbf{B} = 10\bar{1}0$) and corresponding SADPs of (b) $\mathbf{B} = 10\bar{1}0$, (c) $\mathbf{B} = 2\bar{1}\bar{1}0$, (d) BFI ($\mathbf{B} = 0001$) and corresponding SADPs of (e) $\mathbf{B} = 0001$, (f) $\mathbf{B} = 2\bar{1}\bar{1}3$.

although the atom arrangement on the close-packed plane is the same as C14. Since all reflections of C36 structure are common with those of C14 structure, it is possible that some C14 phase could coexist with the C36 in the eutectic region. However, detailed examination of the eutectic region with $\mathbf{B} = 2\bar{1}\bar{1}0$ reveals no phase boundaries inside the compound and uniform lattice fringes perpendicular to [0001] with about 20 Å spacing (as shown in Fig. 3). Considering the larger unit cell of the C36 structure, these facts suggest the absence of C14 phase. Between the eutectic C36 and α-Mg phases, some crystallographic orientation relationships were observed, but there was no regularity within the various regions examined.

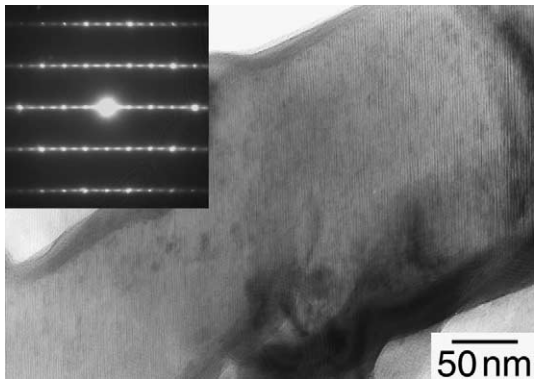

Fig. 3. TEM image of the eutectic region ($\mathbf{B} = 2\bar{1}\bar{1}0$).

Fig. 4 shows a schematic illustration of the crystal structure of C36. Laves phases (C14, C15, C36) consist of the same type of close-packed planes with different stacking sequence [13–16]. There are three types of close-packed planes as shown in Fig. 4(a); the Kagome-net plane consisting of small atoms (Mg or Al) is labeled with A, and two triangular-net planes consisting of either large atoms (Ca) or small atoms are labeled with α and b, respectively. Since the atom positions on α fit into the holes of A, α and A planes always unite together and form a triple layer of αAα. The stacking sequence of close-packed planes is shown in Fig. 4(b) as an atom arrangement on $(2\bar{1}\bar{1}0)$. Displacement of αAα by $a/3\langle 01\bar{1}0\rangle$ makes additional triple layers, designated as βBβ and γCγ. The triangular-net planes of a, b, c are interleaved to fill between upper and lower triple layers. The C36 structure is described by a stacking

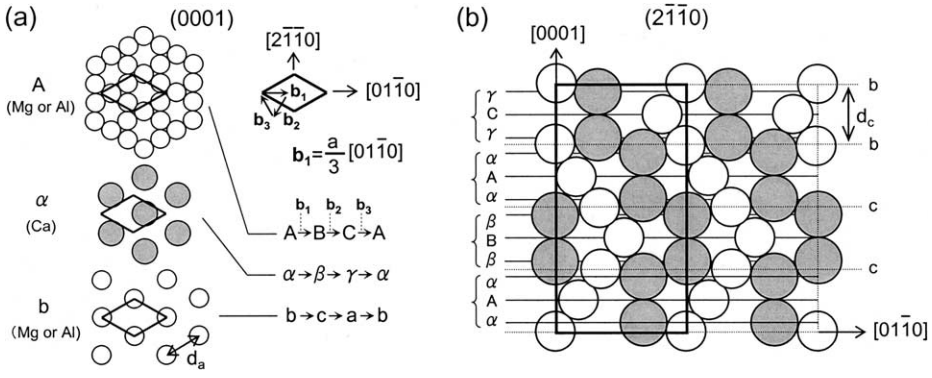

Fig. 4. Crystal structure of C36: (a) three types of close-packed plane: Kagome-net Mg (or Al) plane (A, B, C), triangular-net planes of Ca (α, β, γ) and Mg (or Al) (a, b, c), (b) atom arrangement on $(2\bar{1}\bar{1}0)$ showing the stacking sequence of the closed-packed planes. White and black atoms correspond to Mg (or Al) and Ca, respectively. The unit cell of C36 is indicated by thick lines.

sequence of close-packed planes as [αAα]*c*[βBβ]-*c*[αAα]*b*[γCγ]*b*. Similarly, C14 and C15 are [αAα]*c*[βBβ]*c* and [αAα]*c*[βBβ]*a*[γCγ]*b*, respectively. By regarding a triple layer and an interleaved triangular-net plane (a, b or c) as a quadruple layer, the three Laves phases are described as follows: XYX′Z (C36), XY (C14), XYZ (C15). In this notation, C14 and C15 are hcp and fcc based structures with hexagonality of 100% and 0%, respectively. Since the hexagonality of C36 is 50%, the C36 structure is an intermediate structure between C14 and C15. C36 structures are often observed in alloys containing Cr_2M (M: Nb, Ta, Ti, Zr, Hf) Laves phases [15–20]. They have both C14 and C15 structures at high and low temperatures, respectively, with the C36 structure observed during transformation from C14 to C15 as an intermediate state. Therefore, it is interesting to examine the stability of the C36 phase observed in as-cast AXJ530.

3.2. Stability of the C36 phase

The thermal stability of the C36 phase was examined by applying an aging treatment at 573 K for 360 ks to the as-cast sample. Fig. 5 shows the typical microstructure near grain boundaries following aging. The eutectic intermetallic phase is no longer plate-like and has evolved to be blocky in morphology. However, the original eutectic regions that contained the intermetallic phase still remained surrounding the α-Mg grains and did not break up. Note that fine disc-shaped precipitates are observed in α grains, as indicated by arrowheads. Detailed analysis will be reported elsewhere.

Fig. 6 shows TEM BFIs and SADPs taken in the eutectic region. Fig. 6(a) was taken with $\mathbf{B} = 2\bar{1}\bar{1}0_{C36}$. The eutectic compound exhibits planar interfaces along (0001). In the diffraction pattern, extra reflections are found to exist, as schematically shown in Fig. 6(c) with open circles. They are consistent with the reflections of

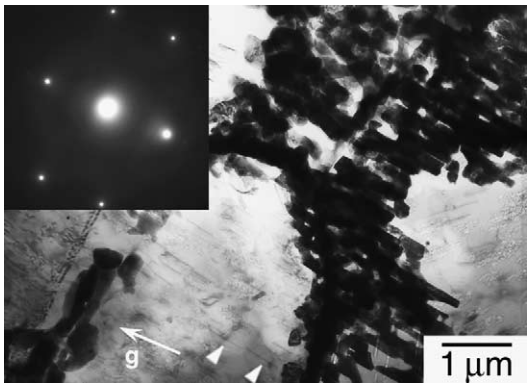

Fig. 5. TEM BFI of the sample aged at 573 K/360 ks ($\mathbf{B} = 4\bar{2}\bar{2}3$).

C15 structure with $\mathbf{B} = 0\,1\,1_{C15}$. Since the reflections of $0\,0\,0\,4_{C36}$ and $\bar{1}\,1\,\bar{1}_{C15}$ coincide, the two phases have the following crystallographic orientation relationship:

$$(0\,0\,0\,1)_{C36} \| (\bar{1}\,1\,\bar{1})_{C15}, [2\bar{1}\bar{1}0]_{C36} \| [0\,1\,1]_{C15}.$$

Detailed observation of the structure within the intermetallic phase reveals the existence of planer faults with several nm intervals on close-packed planes, as shown in Fig. 6(b). The SADP indicates the existence of $\langle 1\,1\,2\rangle\{1\,1\,1\}$ type twin crystals of C15 within C36, as schematically shown in Fig. 6(d). Both twin crystals satisfy the above orientation relationship.

3.3. Phase transition of the eutectic Laves phase

These above results indicate that the C36 phase is metastable at 573 K and that a phase transition to C15 phase takes place during aging. However, why the C36 phase exists in the as-cast state is still in question, and there are two possibilities; one is that the C36 phase is transformed from the original eutectic C14 phase during cooling in the casting process, and the other is that the C36 phase is directly formed by the eutectic transfor-

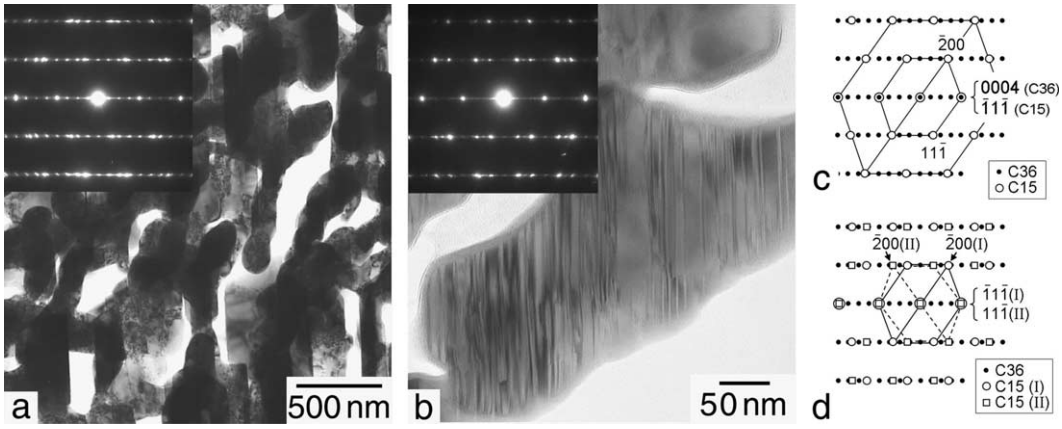

Fig. 6. TEM BFIs and SADPs of the sample aged at 573 K/360 ks ($\mathbf{B} = 2\bar{1}\bar{1}0$): (a) eutectic region; (b) fine twins in (a); (c) and (d) schematic illustrations of SADPs in (a) and (b), respectively.

Table 1
Lattice parameters of Laves phases in as-cast and aged samples, together with the values of stoichiometric phases [21]

	As-cast	573 K/360 ks		Stoichiometry [21]	
	C36	C36	C15	Mg_2Ca (C14)	Al_2Ca (C15)
a/Å	5.96	5.84	8.21	6.22	8.022
c/Å	19.79	18.97	–	10.10	–
c/a	3.32	3.25	–	1.62	–
d_a/Å	5.96	5.84	5.81	6.22	5.67
d_c/Å	4.95	4.74	4.74	5.05	4.63

d_a and d_c correspond to the nearest-neighboring atom spacing on the triangular-net planes and the spacing between the quadruple layers, respectively (Fig. 4).

mation. Further research on Mg–Al–Ca ternary equilibria is necessary to determine the transformation path.

4. Discussion

Table 1 shows lattice parameters of Laves phases in as-cast and aged samples, together with those of stoichiometric Mg_2Ca and Al_2Ca [21]. In order to directly compare the lattice parameters, all values are converted to the nearest-neighboring atom spacing on the triangular-net planes, d_a, and the spacing between the quadruple layers, d_c, as indicated in Fig. 4. The values of d_a and d_c of the stoichiometric Mg_2Ca are $d_a = 6.22$ Å and $d_c = 5.05$ Å, and they are larger than those of Al_2Ca ($d_a = 5.67$ Å, $d_c = 4.63$ Å), because the atomic radius of Mg (1.60 Å) is larger than that of Al (1.43 Å) [22]. The values of the Laves phases observed in this study fall between those of stoichiometric Mg_2Ca and Al_2Ca. In addition, both d_a and d_c are decreased by aging. These facts indicate that the composition of the eutectic compound is close to Mg_2Ca in as-cast state and shifts toward Al_2Ca during aging. Therefore, this phase transition should be caused by the composition change, especially a change in Mg:Al ratio. In the Mg–Ca binary system, the $L \rightarrow \alpha\text{-Mg} + Mg_2Ca$ eutectic temperature is 719 K [23]. At this temperature, the solubility limit of Al in α-Mg is about 12 wt% in the Mg–Al binary system, and decreases to about 6.5 wt% at 573 K [24]. The solubility of Ca is very low, at 0.7 wt% at the most [23]. Thus, in the eutectic region, α-Mg should contain excess Al, and the rejection of excess Al by diffusion during cooling and aging would induce the phase transition of the $(Mg,Al)_2Ca$ phase.

As already shown in Fig. 4, the difference in the crystal structures of Laves phases involves only the stacking sequence of close-packed planes. Therefore, it has been shown that the transition from C36 to C15 is geometrically possible by a shear mechanism that involves syncroshockley dislocations [14,15]. The strong streak in the SADP of C36 in as-cast state (Fig. 2(b) and (c)) and formation of C15 accompanied with fine twins in C36 (Fig. 6(b)) support this mechanism of transformation. Thus, the transformation induced by diffusional redistribution of Mg and Al does not require separate nucleation of the product phase, and proceeds within the interior of the individual intermetallic phase region, although the order of the transformation and the kinetics remain in question. In Mg–Al base alloys without Ca, formation of the $Mg_{17}Al_{12}$ phase by discontinuous precipitation or decomposition of another intermetallic phase at elevated temperatures causes the instability of near-grain boundary microstructure, that is reported to result in the deterioration of creep properties [7,25]. On the other hand, in the present study, as shown in Fig. 5, major morphological change does not occur in the near-grain boundary microstructure, even though the phase constitution has changed. This advantage can apparently be attributed to the utilization of $(Mg,Al)_2Ca$ Laves phases. Further improvement of these alloys might be possible through more detailed understanding of these Laves phases, ternary equilibria and the effect of small additions of Sr.

5. Conclusion

- The crystal structure of the eutectic compound $(Mg,Al)_2Ca$ has been identified as dihexagonal C36 structure in as-cast AXJ530.
- The C36 phase transforms to C15(Al_2Ca) phase during aging at 573 K with the following crystallographic orientation relationship: $(0\,0\,0\,1)_{C36} \| (\bar{1}\,1\,\bar{1})_{C15}$, $[2\bar{1}\bar{1}0]_{C36} \| [011]_{C15}$.
- The change in phase constitution does not result in any major morphological instabilities of the near-grain boundary microstructure.

Acknowledgments

The authors acknowledge the support of NSF Grant No. DMR-0309468. The authors also would like to thank C.J. Torbet and C. Henderson for their assistance

and Dr. B.R. Powell of General Motors for useful discussions and for providing the AXJ530 material.

References

[1] Ninomiya R, Ojiro T, Kubota K. Acta Metall Mater 1995;43:669.
[2] Hollrigl-Rosta F, Just E, Kohler J, Melzer H-J. Light Met Age 1980:22.
[3] Terada Y, Ishimatsu N, Sota R, Sato T, Ohori K. Mater Sci Forum 2003;419–422:459.
[4] Luo AA, Balogh MP, Powell BR. Metall Mater Trans 2002; 33A:567.
[5] Luo AA. Mater Sci Forum 2003;419–422:57.
[6] Pekguleryuz MO, Kaya AA. In: Kainer KU, editor. Magnesium alloys and their applications. Germany: Willey-VCH Verlag GmbH; 2003. p. 74.
[7] Moreno IP, Nandy TK, Jones JW, Allison JE, Pollock TM. Scripta Mater 2003;48:1029.
[8] Ozturk K, Zhong Y, Luo AA, Liu Z-K. JOM 2003;55:40.
[9] Ameioun S, Simak SI, Haussermann U. Inorg Chem 2003;42: 1467.
[10] Catterall JA, Pleasance RJ. J Inst Metals 1957;86:189.
[11] Zhong Y, Luo AA, Sofo JO, Liu Z-K. In: Luo AA, editor. Magnesium techonology 2004. Warrendale, USA. TMS, 2004. p. 317.
[12] Schmid-Fetzer R, Grobner J. In: Kainer KU, editor. Magnesium Alloys and Their Applications. Germany: Willey-VCH Verlag GmbH; 2003. p. 12.
[13] Ferro R, Saccone A. In: Cahn RW, Haasen P, editor. Physical metallurgy, vol. 1, 4th ed. Amsterdam, Netherlands: Elsevier Science; 1996. p. 311.
[14] Hazzledine PM, Pirouz P. Scripta Metall Mater 1993;28:1277.
[15] Kumar KS, Hazzledine PM. Intermetallics 2004;12:763–70.
[16] Kumar KS, Miracle DB. Intermetallics 1994;2:257.
[17] Thoma DJ, Perepezko JH. Mater Sci Eng 1992;A156:97.
[18] Kumar KS, Pang L, Horton JA, Liu CT. Intermetallics 2003;11:677.
[19] Grujicic M, Tangrila S, Cavin OB, Porter WD, Hubbard CR. Mater Sci Eng 1993;A160:37.
[20] Kumar KS, Pang L, Liu CT, Horton J, Kenik EA. Acta Mater 2000;48:911.
[21] Pearson WB. A handbook of lattice spacing and structure of metals and alloys. Pergamon Press; 1958. p. 136, 158.
[22] Ferro R, Saccone A. In: Cahn RW, Haasen P, editor. Physical Metallurgy, vol. 1, 4th ed. Amsterdam, Netherlands: Elsevier Science; 1996. p. 329.
[23] Okamoto H. J Phase Equilib 1998;19:598.
[24] Okamoto H. J Phase Equilib 1998;19:490.
[25] Dargush MS, Dunlop GL, Pettersen K. In: Mordike BL, Kainer KU, editors. Magnesium alloys and their applications. Frankfurt, Germany: Werkstoff-Informationsgesellschaft; 1998. p. 277.